

Semiclassical mechanics of the quadratic Zeeman effect

Kristin D. Krantzman and John A. Milligan

Department of Chemistry and Biochemistry, University of California, Los Angeles, California 90024-1569

David Farrelly

Department of Chemistry and Biochemistry, Utah State University, Logan, Utah 84322-0300

(Received 12 August 1991)

A comprehensive approach to semiclassical quantization of the quadratic Zeeman effect in the hydrogen atom (QZE) is presented which utilizes the connection between the Kepler system and the four-dimensional harmonic oscillator. Past attempts to quantize the QZE have encountered problems associated with singularities arising because of a classical separatrix. Here, a uniform semiclassical quantization scheme that passes smoothly through the separatrix is developed using classical perturbation theory. This method accounts for the topologically distinct kinds of dynamics that arise in the QZE, and provides good estimates of tunneling splittings. Extension to the quantization of arbitrarily-high-order classical perturbation expansions is straightforward.

PACS number(s): 32.60.+i, 03.65.Sq, 31.10.+z

I. INTRODUCTION

The quadratic Zeeman effect in the hydrogen atom (QZE) has for the past decade or so been the subject of an enormous number of experimental and theoretical studies [1–5]. The QZE is an important example of a nonintegrable Hamiltonian that is markedly chaotic in the classical limit. Application of a uniform magnetic field to the hydrogen atom breaks the spherical symmetry, thus destroying angular momentum as a good constant of the motion, although its component along the field direction is preserved. In the opposing limits of very strong or very weak magnetic fields the problem is almost integrable. The dynamics is thus most interesting (and most chaotic) in the mixing region where the magnetic and Coulomb fields are comparable. Sufficiently high Rydberg states can always be found for which this is the case, and most experimental and theoretical studies have focused on understanding this regime. In 1980 Zimmerman, Kash, and Kleppner [6] postulated the existence of an approximate constant of motion based on experimental observations of “quasi-Landau” resonances through the ionization threshold. This constant (denoted Λ) was soon found independently by Solov’ev [7], by Herrick [8], and by Goebel [9]. A fourth independent determination of Λ was made by Reinhardt and Farrelly [10] using classical perturbation theory for the case $m=0$. Λ has been central to almost all subsequent theoretical studies of the QZE, with particular attention having been paid to the quantization of the invariant Λ using semiclassical methods. Most of the issues relating to semiclassical quantization of nonseparable systems and the correspondence limit of quantum mechanics are tied up in the QZE, and it is therefore important that a consistent theoretical picture of the classical and semiclassical mechanics of this problem be developed.

The QZE is an example of a resonant classical system exhibiting topologically distinct types of motion. Reso-

nant systems are much harder to treat semiclassically than nonresonant ones because of the strong distortion of the topology of the trajectories by the resonance and the sensitivity of the dynamics to perturbations, especially close to classical separatrices. (A classical separatrix separates topologically different volumes of phase space.) In such systems it is crucial that the correct unperturbed set of action-angle variables is determined, otherwise nonuniform (singular) quantization formulas result. Consequently much effort has been directed to the general problem of determining the best set of action-angle variables for resonant systems [4,5,11]. Quantizing resonant classical dynamics is akin to performing degenerate quantum perturbation theory, where the correct basis of unperturbed states must first be found if singularities in the perturbation expansion are to be avoided. Resonances in the QZE lead to similar difficulties, giving rise to singular quantization formulas [2,12]. Some studies have avoided the separatrix region, thus minimizing these difficulties, since in the extreme limits of vibrational and rotational motion primitive semiclassical formulas may be used. Nevertheless, the importance of the dynamics in the vicinity of the separatrix necessitates the development of quantization formulas that are uniformly valid through the separatrix. This problem was solved for the special case that $m=0$ previously [12]. In this paper a generally applicable quantization scheme is developed which is applicable to nonzero m values.

The paper is organized as follows: in Sec. II the classical mechanics of the QZE is examined briefly. Section III describes the conversion of the QZE Hamiltonian into that of a four-dimensional [4D] isotropic oscillator with a sextic perturbation. This transformation allows classical perturbation theory to be applied. A transformation to a set of action-angle variables is then introduced. These are used to effect uniform semiclassical quantization, which is described in Sec. IV. Brief conclusions are drawn in Sec. V.

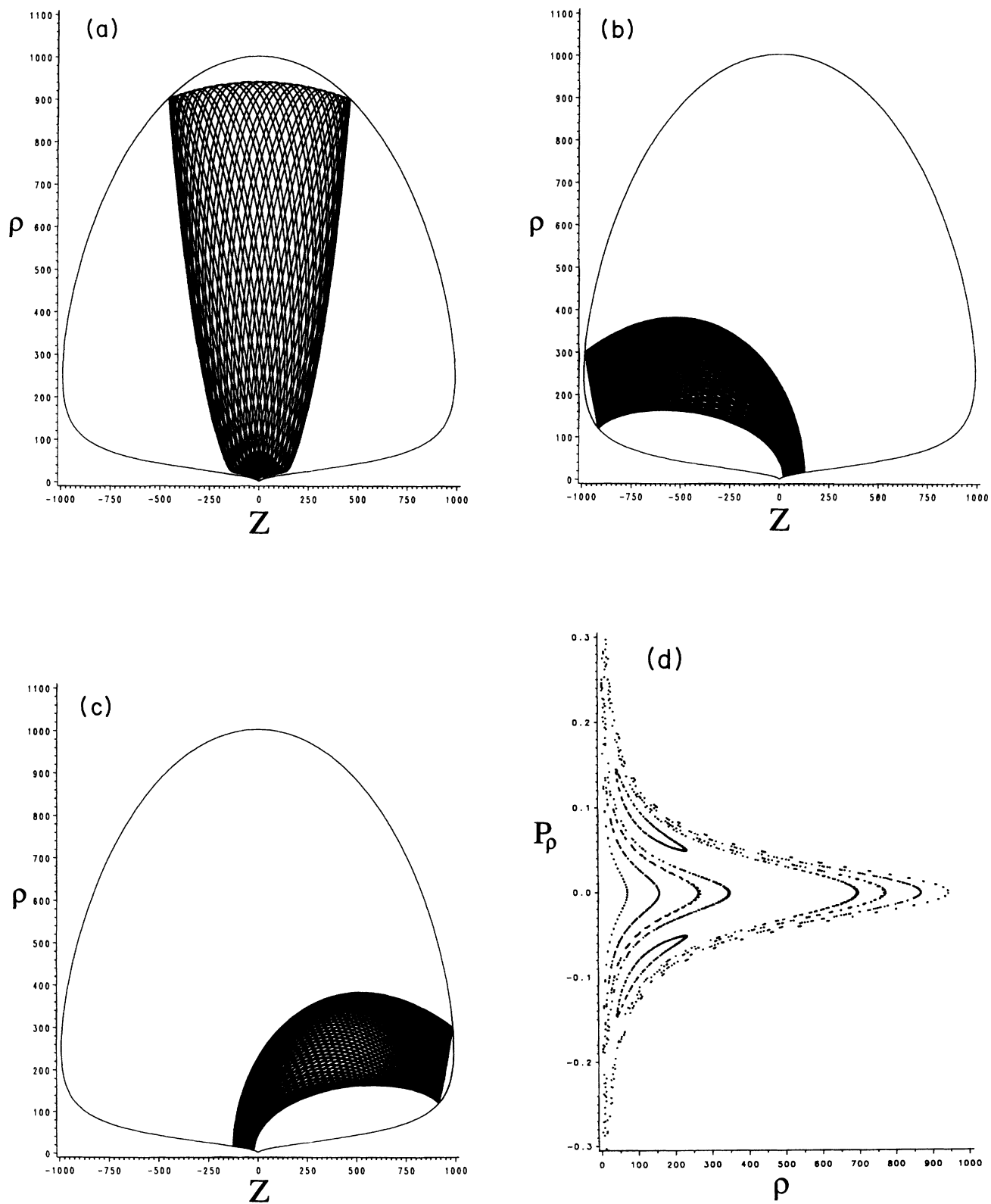


FIG. 1. Classical trajectories and Poincaré surface of section for the QZE in cylindrical coordinates, corresponding to $n=23$, $m=2$, and $\gamma=1.26 \times 10^{-6}$ a.u.; (a) a rotational trajectory with $\Lambda > 0$, (b) a vibrational trajectory with $\Lambda < 0$, and (c) its partner. The vibrational trajectories occur in degenerate pairs related by reflection through the z axis. A composite Poincaré surface of section is shown in (d). It was obtained by running 25 trajectories with randomly chosen initial conditions. The islands correspond to the vibrational trajectories and a separatrix separates the two types of motion.

II. CLASSICAL MECHANICS

In cylindrical coordinates and atomic units ($m_e = e = \hbar = 1$) the Hamiltonian for the QZE is given by

$$H = E + \frac{1}{2}(P_\rho^2 + P_z^2) + \frac{P_\phi^2}{2\rho^2} + \frac{\gamma^2}{8}\rho^2 - \frac{1}{r}, \quad (1)$$

where

$$\rho^2 = x^2 + y^2, \quad r = (\rho^2 + z^2)^{1/2}, \quad (2)$$

$P_\phi = m\hbar$ and the unit of magnetic field is 2.35×10^5 T. The paramagnetic term has been removed by going to a rotating coordinate system [5]. The approximate constant of motion found by Solov'ev [7] and Herrick [8] is given by

$$\Lambda = 4\mathbf{A}^2 - 5\mathbf{A}_z^2, \quad (3)$$

where

$$\mathbf{A} = \frac{1}{\sqrt{(-2H_0)}} \left[\mathbf{p} \times \mathbf{L} - \frac{\mathbf{r}}{r} \right] \quad (4)$$

is the modified Runge-Lenz vector and $H_0 = E_0$ is the unperturbed Kepler energy. The existence of Λ as an approximate constant of motion can be explained in terms of the approximate separability of the Hamiltonian in elliptical cylindrical coordinates on the $O(4)$ sphere within manifolds of constant n [8]. Quantum evaluation of Λ is effected by simultaneously diagonalizing H_0 , L_z , and Λ itself. However, Λ is a first-order-perturbation-theory result and attempts to go to higher orders quantum mechanically become considerably more complicated [13]. On the other hand, classical perturbation methods provide a simple and direct way of calculating very-high-order perturbation expansions [4,10,12]. Λ takes values in the range $(-n^2, 4n^2)$, and the two extremal values correspond to different limiting types of classical motion with a separatrix occurring at $\Lambda = 0$. As illustrated in Fig. 1 trajectories with $\Lambda > 0$ have the full symmetry of the potential and are usually labeled rotational. As Λ approaches its maximum value the trajectories become localized along the ρ axis and correspond to the ridge states of Fano [14] which give rise to the $3/2\hbar\omega$ quasi-Landau resonances [6,15,16]. The second class of trajectories with $\Lambda < 0$ are vibrational in character and occur in degenerate pairs as illustrated in Figs. 1(b) and 1(c). This leads to splittings in the eigenvalue spectrum due to tunneling. The separatrix between the rotational and vibrational types of trajectory occurs at $\Lambda = 0$ and is apparently visible in the Poincaré surface of section shown in Fig. 1(d). For the vibrational states A_z itself is a fairly good constant of motion, making the problem in this limit similar to the Stark effect in hydrogen. In the Hamiltonian (1) the quantum number m appears as a parameter and the dynamics must therefore be examined for each value of m . It is of particular interest to note that, based on first-order classical perturbation theory, the dynamics can be divided into two broad categories depending upon the ratio m/n [17,18]. If $m/n < 1/\sqrt{5}$ both vibrational and rotational trajectories exist, while if $m/n > 1/\sqrt{5}$

only rotational trajectories occur. The separatrix disappears when $m/n = 1/\sqrt{5}$. This is summarized in the surface of section in Fig. 2. This phenomenon has important consequences for quantization; when $m/n < 1/\sqrt{5}$ (the separatrix exists) a quantization formula is needed which goes smoothly from the regime where $\Lambda < 0$ to that where $\Lambda > 0$. When only rotational motion exists then a different quantization formula is needed to treat the single class of rotational states. Richards [17] developed quantization formulas based on classical perturbation theory performed in the Delaunay elements [18,19] which gives good agreement for states far from the separatrix. However, Richard's formulation is singular at the separatrix and is technically invaded in the limit $m = 0$ [17]. It works best when $m/n > 1/\sqrt{5}$ or for the rotational states but does provide good agreement for low-lying vibrational states. The outstanding problem is thus the development of a uniformly valid quantization formula to treat cases where $m/n < 1/\sqrt{5}$ and passage through the separatrix is possible. Stated somewhat differently, Herrick [8] (see also Alhassid, Hinds, and Meschede [20] and Kalnins, Miller, and Winternitz [21]) has shown that the QZE can be viewed as falling between two exact

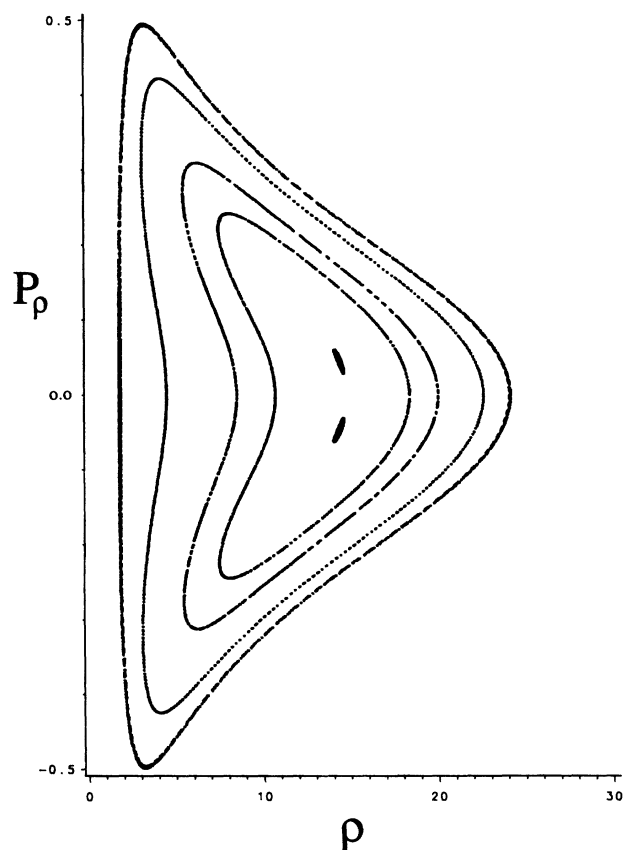


FIG. 2. Composite Poincaré surface of section for the QZE in cylindrical coordinates, with the same parameters as Fig. 1 except $m = n/\sqrt{5}$. The islands have almost disappeared and rotational states dominate phase space.

dynamical-symmetry limits: $O(4) \supset O(3)_\lambda \supset O(2)$ and $O(4) \supset O(2) \otimes O(2)$. [The subscript “ λ ” in $O(3)_\lambda$ indicates that the generators of the Lie algebra are those of a nonstandard angular momentum having components (A_x, A_y, L_z) .] As the value of m increases the former dynamical chain becomes more appropriate. The next section describes how classical perturbation theory can be applied to the QZE together with a transformation to action-angle variables which makes uniform semiclassical quantization possible.

III. TRANSFORMATION INTO FOUR DIMENSIONS

The tack taken is to make use of the well-known connection between the hydrogen atom and a four-dimensional isotropic harmonic oscillator. This correspondence may be established either by using the Kustaanheimo-Stiefel transformation [22–24] (KS) or via group theory. Each has its merits. The KS transformation, originally designed to regularize the classical motion, allows any perturbation to be written in terms of the canonical coordinates and momenta of the 4D oscillator. This is necessary in order to apply classical perturbation theory. However, the group-theoretical description gives a deeper perspective which enables the transformation to good action-angle variables to be made. The connection between the Kepler problem and a 4D oscillator is due to the existence of the angular momentum \mathbf{L} and the Laplace-Runge-Lenz vector \mathbf{A} as constants of motion which are related to each other through the requirement $\mathbf{L} \cdot \mathbf{A} = 0$.

The KS transformation starts by relating the original Cartesian coordinates to a set of coordinates in a 4D space using

$$\mathbf{r} = \mathbf{T}\mathbf{u}, \quad (5)$$

where

$$\mathbf{T} = \begin{pmatrix} u_1 & -u_2 & -u_3 & u_4 \\ u_2 & u_1 & -u_4 & -u_3 \\ u_3 & u_4 & u_1 & u_2 \\ u_4 & -u_3 & u_2 & -u_1 \end{pmatrix} \quad (6)$$

and $\mathbf{u} = (u_1, u_2, u_3, u_4)$, $\mathbf{r} = (x_1, x_2, x_3)$, and \mathbf{T} satisfies the orthogonality relation

$$\mathbf{T}'\mathbf{T} = \mathbf{T}\mathbf{T}' = |\mathbf{u}^2|. \quad (7)$$

In Eq. (7),

$$|\mathbf{u}^2| = u_1^2 + u_2^2 + u_3^2 + u_4^2. \quad (8)$$

The two sets of coordinates are related explicitly by the following:

$$x_1 = z = u_1^2 - u_2^2 - u_3^2 + u_4^2, \quad (9)$$

$$x_2 = y = 2(u_1 u_2 - u_3 u_4), \quad (10)$$

$$x_3 = x = 2(u_1 u_3 + u_2 u_4). \quad (11)$$

The dynamical variables can be related by using the momenta \mathbf{p}_u conjugate to \mathbf{u} ,

$$\mathbf{p}_u = {}^t(p_1, p_2, p_3, p_4) \quad (12)$$

for which the following constraint holds:

$$u_1 p_4 - u_4 p_1 + u_3 p_2 - u_2 p_3 = 0, \quad (13)$$

and

$$\sum_{i=1}^3 p_{x_i} d_{x_i} = \sum_{i=1}^4 p_i d_{u_i}. \quad (14)$$

Thus

$$\mathbf{p}_x = \frac{1}{2r} \mathbf{T} \mathbf{p}_i, \quad (15)$$

where

$$\mathbf{p}_x = {}^t(p_{x_1}, p_{x_2}, p_{x_3}). \quad (16)$$

In view of Eq. (13) the system is subject to the constraint

$$P_\phi = m = u_1 p_4 - u_4 p_1 = u_3 p_2 + u_2 p_3 \quad (17)$$

which converts the QZE Hamiltonian into

$$H = \frac{1}{8r} \mathbf{p}_u^2 - \frac{1}{|\mathbf{u}|^2} + \frac{\gamma^2}{2} (u_1^2 + u_4^2)(u_2^2 + u_3^2). \quad (18)$$

This, in turn, can be converted into a system of four coupled harmonic oscillators by making the transformation to a new time variable s (regularization),

$$\frac{dt}{ds} = 4r = 4|\mathbf{u}|^2. \quad (19)$$

Multiplying through by $4r$ gives the Hamiltonian

$$K = 4 = \frac{1}{2}(\mathbf{p}_u^2 + \omega^2 |\mathbf{u}|^2) + 2\gamma^2 |\mathbf{u}|^2 (u_1^2 + u_4^2)(u_2^2 + u_3^2), \quad (20)$$

where

$$\omega^2 = -8E. \quad (21)$$

Scaling the coordinates and momenta

$$u_i \rightarrow \frac{u_i}{\sqrt{\omega}}, \quad p_i \rightarrow \sqrt{\omega} p_i, \quad (22)$$

yields

$$K = \frac{4}{\omega} = \frac{1}{2}(\mathbf{p}_u^2 + |\mathbf{u}|^2) + 2\frac{\gamma^2}{\omega^4} |\mathbf{u}|^2 (u_1^2 + u_4^2)(u_2^2 + u_3^2). \quad (23)$$

In the limit of $\gamma = 0$ the problem is thus a four-dimensional isotropic oscillator. An alternative route to the oscillator picture makes use of the components of \mathbf{L} and \mathbf{A} that generate the Lie algebra of the group $SO(4)$ [isomorphic to $SO(3) \otimes SO(3)$] [25]. The generators of $SO(3) \otimes SO(3)$ are two angular momenta \mathbf{J} and \mathbf{K} which are related to the $SO(4)$ generators by

$$\mathbf{J} = \frac{\mathbf{L} + \mathbf{A}}{2}, \quad \mathbf{K} = \frac{\mathbf{L} - \mathbf{A}}{2}. \quad (24)$$

The transformation of the unperturbed problem proceeds

by writing the components of \mathbf{J} and \mathbf{K} in terms of the classical equivalents of boson operators [25], viz.,

$$\begin{aligned} J_1 &= \frac{a_1^\dagger a_2 + a_1 a_2^\dagger}{2}, \\ J_2 &= \frac{a_1^\dagger a_2 - a_1 a_2^\dagger}{2i}, \end{aligned} \quad (25)$$

$$\begin{aligned} J_3 &= \frac{a_1^\dagger a_1 - a_2^\dagger a_2}{2}, \\ K_1 &= \frac{a_3^\dagger a_4 + a_3 a_4^\dagger}{2}, \\ K_2 &= \frac{a_3^\dagger a_4 - a_3 a_4^\dagger}{2i}, \\ K_3 &= \frac{a_3^\dagger a_3 - a_4^\dagger a_4}{2}. \end{aligned} \quad (26)$$

The passage to the harmonic-oscillator picture is accomplished by associating Cartesian coordinates with the boson operators

$$a_i = (Q_i + iP_i)/\sqrt{2}, \quad a_i^\dagger = (Q_i - iP_i)/\sqrt{2}. \quad (27)$$

This eventually results in the Hamiltonian of an isotropic four-dimensional oscillator [26]

$$K_0 = \frac{4}{\omega} = \frac{1}{2}(P_1^2 + P_2^2 + P_3^2 + P_4^2 + Q_1^2 + Q_2^2 + Q_3^2 + Q_4^2) \quad (28)$$

together with the constraint

$$\frac{1}{2}(P_1^2 + P_2^2 + Q_1^2 + Q_2^2) = \frac{1}{2}(P_3^2 + P_4^2 + Q_3^2 + Q_4^2). \quad (29)$$

The energy is quantized using the relation [27]

$$K_0 = \frac{2}{\sqrt{-2E}} = N + 2 = 2n, \quad (30)$$

where $n = (N/2 + 1)$ is the principal (hydrogenic) quantum number, and

$$N = N_1 + N_2 + N_3 + N_4. \quad (31)$$

Here N_i is the quantum number associated with the i th oscillator ($i=1,2,3,4$) and takes values $0,1,2,\dots$. In terms of the oscillator quantum numbers the constraint (29) becomes

$$N_1 + N_2 - N_3 - N_4 = 0, \quad (32)$$

which guarantees that N is even and thus that n is integer. This is equivalent to requiring that $J^2 = K^2$, i.e., the "square representation." The results so far apply only to the unperturbed system and this approach has the disadvantage that it provides no easy way to convert the perturbation in Eq. (1) into the oscillator coordinates and momenta. The difference between the KS constraint (17) and Eq. (29) is related to the nonuniqueness of Eqs. (25)–(27), i.e., the phase-space coordinates in the KS transformation are different from those in Eqs. (25)–(27) but are related to them by a canonical transformation which can best be thought of as a rotation in phase space.

This may be understood by thinking of the problem as an $SU(2) \otimes SU(2)$ system. Each of the angular momenta \mathbf{J} and \mathbf{K} has components J_i and K_i ($i=1,2,3$) which each generate the Lie algebra of $SU(2)$. Each of these systems specifies a sphere of radius J^2 and K^2 , respectively, with the J_i and the K_i serving as Cartesian coordinates to label points on the surface of the sphere. Consequently, the J_i and the K_i may be rotated arbitrarily in three-dimensional space provided their commutation relations remain unaffected. In essence the KS transformation puts one in a phase space which has been rotated as compared to that in Eq. (28). The straightforward connection between the components of \mathbf{A} and \mathbf{L} and the J_i and the K_i [Eq. (24)] makes the P_i and Q_i ultimately more convenient to work with than the p 's and u 's of the KS transformation. A transformation between the two sets of coordinates is given by the following:

$$\begin{aligned} u_1 &= \frac{-(Q_1 + P_4)}{\sqrt{2}}, & p_1 &= \frac{Q_4 - P_1}{\sqrt{2}}, \\ u_2 &= \frac{Q_3 - P_2}{\sqrt{2}}, & p_2 &= \frac{Q_2 + P_3}{\sqrt{2}}, \\ u_3 &= \frac{-(Q_2 - P_3)}{\sqrt{2}}, & p_3 &= \frac{-(Q_3 + P_2)}{\sqrt{2}}, \\ u_4 &= \frac{-(Q_4 + P_1)}{\sqrt{2}}, & p_4 &= \frac{Q_1 - P_4}{\sqrt{2}}. \end{aligned} \quad (33)$$

This transforms Eq. (17) into Eq. (29) while preserving Eq. (28). The KS transformation has the practical advantage that any perturbation expressed only in terms of the original Cartesian coordinates is expressible in terms of the coordinates u_i . In contrast, the canonical transformation (33) mixes coordinates and momenta in the perturbation. It is therefore simpler to perform classical perturbation theory in the KS coordinates and then to apply the transformation (33). The Hamiltonian (23) was converted into normal form [12,18] using classical perturbation theory through sixth order in the magnetic field. The resulting expression contained thousands of terms but agreed with the results of Kuwata, Harada, and Hasegawa [24] where comparison was possible. After generating the normal form the transformation (33) was applied. All of the transformations were effected by means of the symbolic manipulation program SMP. The next step is to go to action-angle variables in order to effect quantization. Based on the examination of the classical dynamics and quantization of the $m=0$ case [12], a transformation is looked for which will convert the normal form into an expression containing the action variables n and m together with A_z and its conjugate angle ϕ_{A_z} . A lone angle is expected to survive because the problem is resonant. The initial transformation to action-angle variables is the following:

$$Q_i = \sqrt{2I_i} \sin \phi_i, \quad P_i = \sqrt{2I_i} \cos \phi_i, \quad (34)$$

where $i=1,2,3,4$. Two further transformations are then performed in order to eliminate all but one angle.

First,

$$\begin{aligned}
I_1 &= \frac{I_a + I_b}{2}, \quad \phi_1 = \phi_a + \phi_b, & I_b &= m + A_z, \quad \phi_b = \frac{\phi_m + \phi_{A_z}}{2} \\
I_2 &= \frac{I_a - I_b}{2}, \quad \phi_2 = \phi_a - \phi_b, & I_d &= m - A_z, \quad \phi_d = \frac{\phi_m - \phi_{A_z}}{2}
\end{aligned} \tag{35}$$

[the constraint (32) requires that $I_a = I_c = n$]. This converts the normal form K^{NF} (through second order in the field) into

$$K^{\text{NF}} = \frac{4}{\omega} = 2n - \frac{\gamma^3}{\omega^4} \Xi(n, m; A_z, \phi_{A_z}), \tag{37}$$

and, second

where,

$$\begin{aligned}
\Xi(n, m; A_z, \phi_{A_z}) &= -6n A_z^2 - 2nm^2 + 6n^3 - 4n \{ [n^2 - (m + A_z)^2] + [n^2 - (m - A_z)^2] \}^{1/2} \\
&\quad + 8n \{ [n^2 - (m + A_z)^2] [n^2 - (m - A_z)^2] \}^{1/2} \cos^2(\phi_{A_z})
\end{aligned} \tag{38}$$

and the constant of the motion Λ is given by the expression

$$\Lambda = 2 \{ [n^2 - (m + A_z)^2] [n^2 - (m - A_z)^2] \}^{1/2} \cos(2\phi_{A_z}) - 3 A_z^2 - 2m^2 + 2n^2. \tag{39}$$

Transformation of Eqs. (25) and (26) into these variables leads to the results

$$\begin{aligned}
J_3 + K_3 &= m, \\
J_3 - K_3 &= A_z,
\end{aligned} \tag{40}$$

as expected in view of Eq. (24). J_3 and K_3 can each take values in the range $(-n/2, n/2)$ which gives

$$|A_z| \leq |n - |m||. \tag{41}$$

Importantly, the normal form was found to depend only on the angle ϕ_{A_z} which establishes its integrability. The sequence of transformations described also allows explicit expressions for x, y, z and p_x, p_y, p_z to be obtained in terms of the sets of action-angle variables (n, ϕ_n) , (m, ϕ) , and (A_z, ϕ_{A_z}) . This completes the derivation of the normal form and its transformation to action-angle variables.

Through second order in the magnetic field, quantization of the normal form is equivalent to quantization of Λ [see Eq. (39)]. Quantization of the full normal form proceeds in essentially the same way but requires considerably more numerical effort. Contour plots of Λ as a function of A_z and ϕ_{A_z} obtained by using Eq. (39) are shown in Fig. 3. These plots can be interpreted as Poincaré surfaces of section for $\phi_n = \text{const}$ and resemble closely the results of numerical investigations [28]. It is important to note that the plots in Fig. 3 are based on an analytical expression for Λ . When $m/n < 1/\sqrt{5}$ the plots resemble a twofold hindered rotor and if $m=0$ Λ takes its full range of values $(-n^2, 4n^2)$. A curious feature of the transformation is that the librational states of the rotor which lie in the wells correspond to rotational ($\Lambda > 0$) states of the original Hamiltonian (1). Conversely, the original vibrational states ($\Lambda < 0$) have been mapped onto rotational states of the rotor. This might

seem puzzling: however, the original vibrational trajectories are localized in disjoint regions of phase space and the transformation to regularized coordinates is thus expected to map these trajectories into localized states of the oscillator. Local modes in the oscillator picture are those best conserving the rotor action [29], i.e., the rotational states of the rotor (which almost conserve A_z). The oscillator normal-mode states in the wells ($\Lambda > 0$) become the ridge states of Fano [14,30] as Λ approaches its maximum value. The stability of these states against "falling" off of the ridge can be understood by noting that they exist at the bottom of a well in action-angle space. As m is increased the volume of phase space supporting rotational states shrinks until $m/n = 1/\sqrt{5}$ when they, along with the separatrix, have vanished altogether. This picture assumes that the higher-order terms in the normal form are negligible compared to those which are second-order in the field. This has been verified numerically in this limit. As the field is increased the higher-order terms become more important and begin to distort this picture. The present analysis is restricted to the case that only second-order terms need be retained.

An interesting way to examine the structure of phase space is to use the idea of a rotational-energy surface (RES) in which each of the SU(2) generators is associated with a component of an angular momentum [4,31-33]. A RES is usually a plot of the energy of a system as a function of the direction of the angular momentum vector. The components of angular momentum are interpreted as Cartesian coordinates of a position vector whose length is equal to the energy which is plotted radially outwards. This was done in Refs. [4] and [33] for the $m=0$ QZE (see also Ref. [34]). The phase-space plots of Λ shown in Fig. 3 indicate that the hindered rotor picture persists provided $m/n < 1/\sqrt{5}$. It is therefore illuminating to construct a RES based on the generalized angular momentum \mathbf{S} defined as

$$\begin{aligned}
 S^2 &= \frac{(n^2 - |m|^2)}{4}, \\
 S_1 &= \frac{A_z}{2}, \\
 S_2 &= (S^2 - S_1^2)^{1/2} \sin \theta_z, \\
 S_3 &= (S^2 - S_1^2)^{1/2} \cos \theta_z,
 \end{aligned}
 \tag{42}$$

where

$$\theta_z = 2\phi_{A_z}. \tag{43}$$

Interpreting Λ as the “energy” (i.e., the radius) results in the RES's shown in Fig. 4. For vibrational states Λ takes negative values and therefore the radius has been offset by the minimum value of Λ for each RES. Each

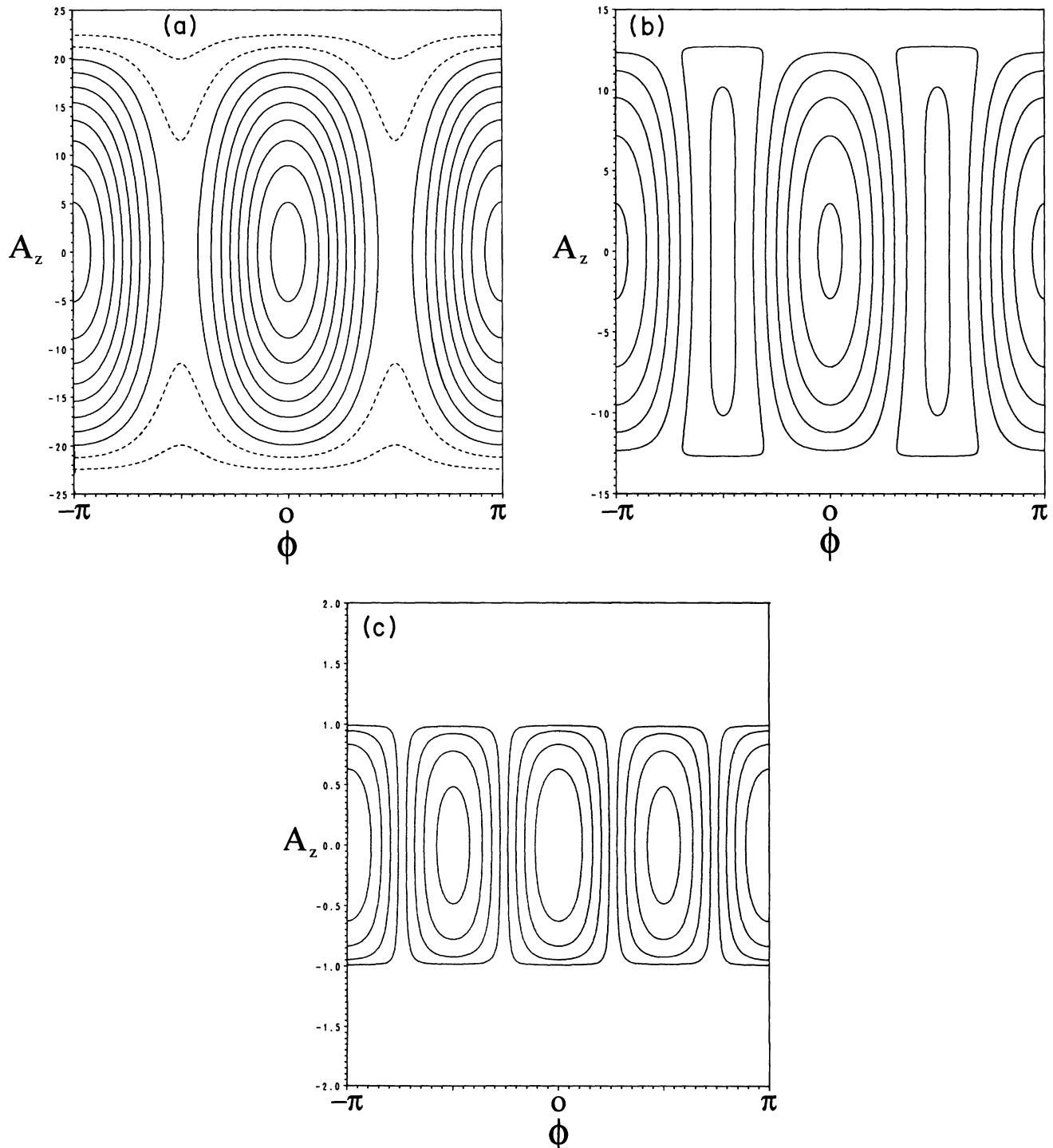


FIG. 3. Level curves of Λ as A_z and ϕ_{A_z} are varied at several values of m with $n = 23$. The dashed curves indicate where Λ is negative, i.e., the vibrational states of the QZE. In (a) $m = 0$, in (b) $m = n/\sqrt{5}$, and in (c) $m = 22$.

RES has been shaded to reflect regions where Λ is negative, i.e., regions corresponding to vibrational states. The rotational states are localized around the lobes of the RES's, while the vibrational states lie in the dimples and are separated by a classical separatrix. The separatrix is evident in Fig. 4(a) upon examining the contours superimposed on the surface. The contours are level curves corresponding to equal values of $|\Lambda|$. As m is increased the region of phase space supporting vibrational states shrinks until m passes through the value $m = n/\sqrt{5}$ when they disappear altogether. This manifests itself as the separatrix first shrinking and then sliding around the RES. The variation in S_1 as a function of θ_z is obtained by tracing θ_z along the level curves. The orientation is maintained between the figures and the separatrix has just vanished in Fig. 4(c). The separatrix which appears to grow in again as m increases beyond $m = n/\sqrt{5}$ is because of the mapping of the problem onto an oscillator. The new states apparently lying in the dimples in Fig. 4(d) do not correspond to real QZE states. A pseudocolored version of Fig. 4(a) in which the variation in the action A_z as a function of its conjugate angle is shown in Ref. [4].

IV. QUANTIZATION OF THE NORMAL FORM

Once the transformation to action-angle variables has been accomplished, uniform semiclassical quantization of Λ is possible. (The quantum evaluation of Λ has been described by Grozdanov and Taylor [35].) There have been a number of previous semiclassical attempts to quantize the QZE [2,5,12,17,24,33,36,37]; ours differs in that it gives a uniform semiclassical quantization of the problem valid for arbitrary $m/n < 1/\sqrt{5}$. For $m/n > 1/\sqrt{5}$ an adequate quantization formula already exists in terms of the Delaunay actions and provides excellent agreement with quantum results [17]. In the case that $m/n < 1/\sqrt{5}$ the problem is essentially a twofold hindered rotor (see Fig. 3) for which the appropriate uniform semiclassical quantization formula (including tunneling) is [38,39]

$$\alpha - \Phi(\epsilon) = k\pi \pm \tan^{-1}[\exp(-\pi\epsilon)] ,$$

$$k = 1, 2, \dots, (n - |m|) \quad (44)$$

where

$$\alpha = \int_a^b A_z(n, m, \Lambda; \phi_{A_z}) d\phi_{A_z} \quad (45)$$

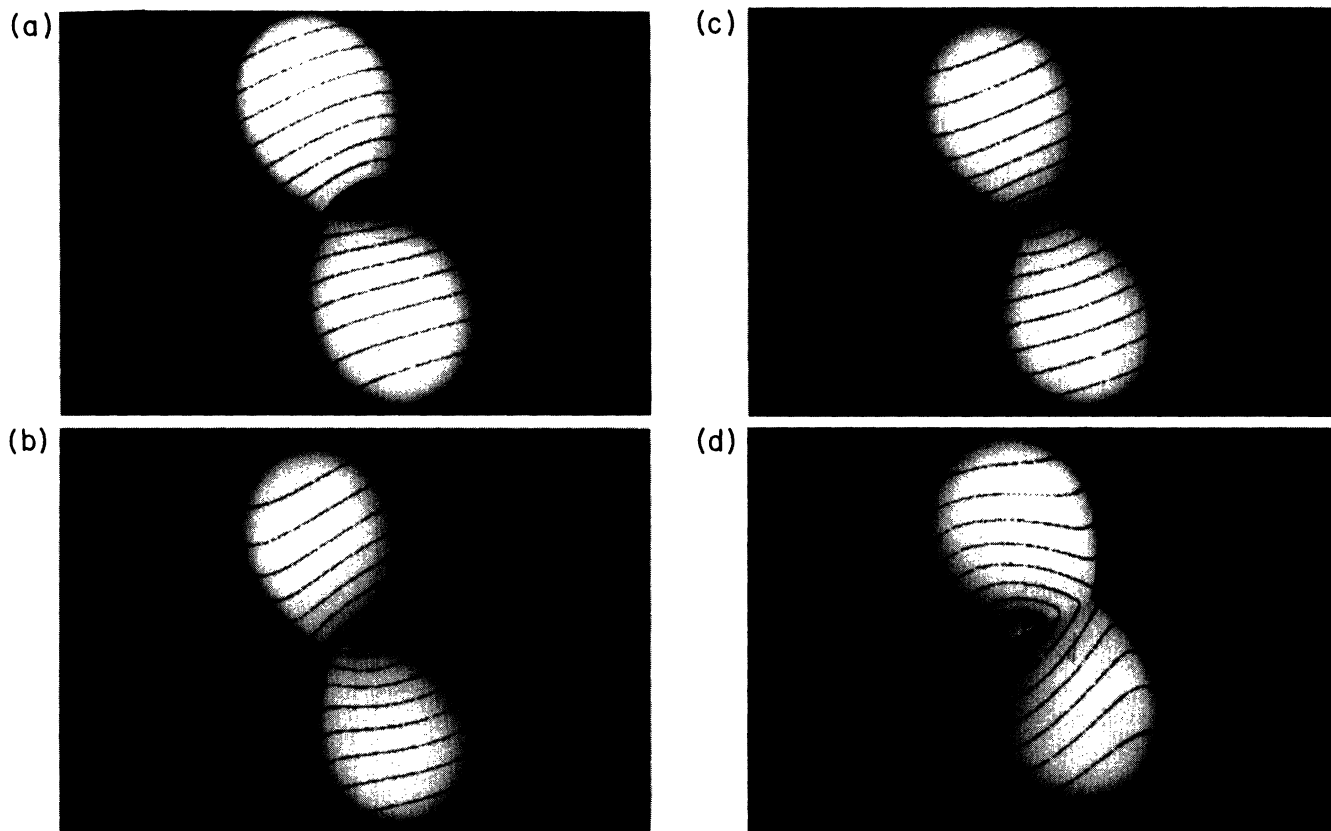


FIG. 4. Rotational energy surfaces corresponding to $n=23$ and (a) $m=0$, (b) $m=4$, (c) $m = n/\sqrt{5}$, and (d) $m=22$. The surfaces have been shaded gray to indicate where Λ is negative. The Cartesian coordinate system is defined as follows using (a). One axis runs along the long axis of the body. A second axis around which the angle θ_z varies [see Eq. (43)] emanates from the dimple (shaded gray) in (a). The third axis is orthogonal to these. The orientation is kept constant between figures. The contours are level curves corresponding to the intersection of the RES with spheres of progressively increasing radii equal to $|\Lambda|$.

TABLE I. Quantum-mechanical [5,35] λ^{QM} and semiclassical λ^{SC} eigenvalues of $\lambda = \Lambda/n^2$ for $n = 23$ and $m = 0$.

k^\pm	λ^{QM}	λ^{SC}	k^\pm	λ^{QM}	λ^{SC}
22 ⁺	-0.815 18	-0.811 77	12 ⁻	0.659 82	0.662 49
22 ⁻	-0.815 18	-0.811 77	11 ⁻	0.858 67	0.861 21
20 ⁺	-0.474 47	-0.471 03	10 ⁻	1.075 54	1.077 86
20 ⁻	-0.474 45	-0.471 01	9 ⁻	1.309 82	1.312 16
18 ⁺	-0.191 24	-0.187 67	8 ⁻	1.561 67	1.563 92
18 ⁻	-0.188 60	-0.185 09	7 ⁻	1.830 84	1.833 02
16 ⁺	-0.006 50	-0.002 71	6 ⁻	2.117 24	2.119 36
	Separatrix		5 ⁻	2.420 82	2.422 87
16 ⁻	0.050 73	0.054 13	4 ⁻	2.741 15	2.743 50
15 ⁻	0.179 02	0.179 87	3 ⁻	3.079 30	3.081 22
14 ⁻	0.317 83	0.320 83	2 ⁻	3.434 14	3.435 99
13 ⁻	0.479 35	0.482 14	1 ⁻	3.806 02	3.807 78

and

$$\pi\epsilon = - \int_b^c |A_z(n, m, \Lambda; \phi_{A_z})| d\phi_{A_z} \quad (46)$$

and the classical turning points (a, b, c) are complex for states lying above the barrier tops. The quantum correction function is an antisymmetric function of its argument and is defined

$$\Phi(\epsilon) = \epsilon + \arg\Gamma(\frac{1}{2} + i\epsilon) - \epsilon \ln|\epsilon|. \quad (47)$$

Note that the states are split due to quantum tunneling and must be labeled according to the quantum number k together with $+$ or $-$ (i.e., k^+ or k^-), depending upon which was taken in Eq. (44). The actual quantization is accomplished by solving Eq. (39) to give A_z as a function of its arguments which are indicated explicitly in Eqs. (45) and (46). (To quantize the full normal form to higher order, it would have to be inverted numerically to give A_z .) Application of these formulas provides all of the

states of the rotor but not all of these correspond to states of the QZE. On going from the original Kepler problem to the 4D oscillator the size of phase space was clearly increased, i.e., only some fraction of the oscillator states match up with states of the hydrogen atom. This manifests itself as restrictions on the values that k may take in Eq. (44). In fact half of the possible eigenstates of the rotor are ruled out giving $n - |m|$ states altogether. For *vibrational* states lying well above the barrier tops an approximate quantization rule is

$$\alpha = \int_0^\pi A_z(n, m, \Lambda; \phi_{A_z}) d\phi_{A_z} = k\pi \quad (48)$$

or roughly, $A_z = k$. By considering Eq. (40) it is clear that if m is even then J_3 and K_3 must either both be odd or both be even. In each case this means that $(J_3 - K_3)$ is even. Thus for m even the quantum number k must be even, and similarly if m is odd then k must be odd also. This rule applies, however, only to the Zeeman vibrational states where A_z is itself an approximate quantum num-

TABLE II. Quantum [5,35] λ^{QM} and semiclassical λ^{SC} eigenvalues of $\lambda = \Lambda/n^2$ for $n = 23$ and $m = 1$. The numbers in square brackets are the powers of 10 by which the entrant is multiplied.

k^\pm	λ^{QM}	λ^{SC}	k^\pm	λ^{QM}	λ^{SC}
21 ⁺	-0.642 08	-0.638 66	11 ⁻	0.852 81	0.854 76
21 ⁻	-0.642 08	-0.638 66	10 ⁻	1.069 27	1.071 70
19 ⁺	-0.327 67	-0.324 19	9 ⁻	1.303 41	1.305 74
19 ⁻	-0.327 46	-0.323 99	8 ⁻	1.555 04	1.557 29
17 ⁺	-0.861 35[-1]	-0.823 60[-1]	7 ⁻	1.824 02	1.826 20
17 ⁻	-0.694 97[-1]	-0.659 93[-1]	6 ⁻	2.110 27	2.112 38
	Separatrix		5 ⁻	2.413 70	2.415 75
16 ⁻	0.675 89[-1]	0.712 24[-1]	4 ⁻	2.734 28	2.736 26
15 ⁻	0.171 83	0.175 03	3 ⁻	3.071 96	3.073 88
14 ⁻	0.313 65	0.313 60	2 ⁻	3.426 71	3.428 55
13 ⁻	0.474 27	0.477 08	1 ⁻	3.788 50	3.800 26
12 ⁻	0.654 33	0.656 99			

TABLE III. Quantum-mechanical $[5,35]$ λ^{QM} and semiclassical λ^{SC} eigenvalues of $\lambda = \Lambda/n^2$ for $n=23$ and $m=2$. The numbers in square brackets are the powers of 10 by which the entrant is multiplied.

k^\pm	λ^{QM}	λ^{SC}	k^\pm	λ^{QM}	λ^{SC}
20 ⁺	-0.488 38	-0.484 92	10 ⁻	1.050 82	1.053 24
20 ⁻	-0.488 37	-0.484 91	9 ⁻	1.284 19	1.286 51
18 ⁺	-0.203 19	-0.199 61	8 ⁻	1.535 16	1.537 40
18 ⁻	-0.201 24	-0.197 72	7 ⁻	1.803 58	1.805 75
16 ⁺	-0.142 80[-1]	-0.103 50[-1]	6 ⁻	2.089 34	2.091 44
Separatrix					
16 ⁻	0.372 21[-1]	0.406 34[-1]	5 ⁻	2.392 35	2.394 40
15 ⁻	0.164 04	0.163 30	4 ⁻	2.712 56	2.714 54
14 ⁻	0.299 75	0.302 75	3 ⁻	3.049 92	3.051 84
13 ⁻	0.459 17	0.461 94	2 ⁻	3.404 39	3.406 23
12 ⁻	0.637 88	0.640 54	1 ⁻	3.777 59	3.777 69
11 ⁻	0.835 28	0.837 80			

ber. These states may be labeled $|n, k^\pm\rangle$ and the difference in energy between the + and - states corresponds to the tunneling splitting. Below the barrier tops (i.e., inside the separatrix) A_z is not conserved, even approximately, and the rotational states of the QZE are not split by tunneling. The subseparatrix states of the hindered rotor occur as symmetric and antisymmetric pairs. The states of the rotor which match up with the QZE states are the symmetric members of each pair of states. In the limit of no tunneling both members of a pair of states localized in the wells must map back into the same rotational state of the original QZE. In the limit of extreme rotational motion which corresponds to motion in the $x-y$ plane the trajectories are invariant to reflection through the x and y axes. Therefore, upon inclusion of tunneling in the rotor picture only the symmetric states below the barrier tops must be taken. Most importantly, this procedure yields a perfectly well-behaved quantization formula giving accurate results for all states, including those close to the separatrix. Results are presented in Tables I-III for the $n=23$ manifold with $m=0, 1, 2$. In

all cases excellent agreement with quantum results is obtained, even for states lying close to, or straddling, the separatrix. This provides direct numerical confirmation of the analysis presented.

V. CONCLUSIONS

A comprehensive approach to semiclassical quantization of the QZE has been presented. Past attempts to quantize the QZE have encountered singularities associated with the classical separatrix. To avoid these problems a variety of piecewise or *ad hoc* quantization formulas have been proposed. In this paper a uniformly valid quantization scheme was developed which passes through the separatrix in a completely smooth and singularity free way. This formula accounts for the topologically distinct kinds of dynamics which arise in the QZE and provides good estimates of splittings between degenerate vibrational trajectories. Extension of this approach to quantization of very-high-order classical perturbation expansions is straightforward.

- [1] H. Friedrich and D. Wintgen, *Phys. Rep.* **183**, 37 (1989).
 [2] H. Hasegawa, M. Robnik, and G. Wunner, *Prog. Theor. Phys. Suppl.* **98**, 198 (1989).
 [3] A. Holle, J. Main, G. Wiebusch, H. Rottke, and K. H. Welge, *Phys. Rev. Lett.* **61**, 161 (1987).
 [4] T. Uzer, D. Farrelly, J. A. Milligan, P. E. Raines, and J. P. Skelton, *Science* **242**, 42 (1991).
 [5] S. Saini and D. Farrelly, *Phys. Rev. A* **36**, 3556 (1987).
 [6] M. L. Zimmerman, M. L. Kash, and D. Kleppner, *Phys. Rev. Lett.* **45**, 1092 (1980).
 [7] E. A. Solov'ev, *Pis'ma Zh. Eksp. Teor. Fiz.* **34**, 278 (1981) [*JETP Lett.* **54**, 265 (1981)]; *Zh. Eksp. Teor. Fiz.* **82**, 1762 (1982) [*Sov. Phys.—JETP* **55**, 1017 (1982)].
 [8] D. R. Herrick, *Phys. Rev. A* **26**, 323 (1982).
 [9] C. Goebel (unpublished).
 [10] W. P. Reinhardt and D. Farrelly, *J. Phys. (Paris) Colloq.* **43**, C2 (1982).
 [11] D. Farrelly, *J. Chem. Phys.* **85**, 2119 (1986).
 [12] D. Farrelly and K. D. Krantzman, *Phys. Rev. A* **43**, 1666 (1991).
 [13] W. Janke and H. Kleiner, *Phys. Rev. A* **42**, 2792 (1990).
 [14] U. Fano, *J. Phys. B* **13**, L519 (1980).
 [15] Chun-ho Iu, G. R. Welch, M. M. Kash, L. Hsu, and D. Kleppner, *Phys. Rev. Lett.* **62**, 1975 (1989).
 [16] G. R. Welch, M. M. Kash, Chun-ho Iu, L. Hsu, and D. Kleppner, *Phys. Rev. Lett.* **63**, 1133 (1989).
 [17] D. Richards, *J. Phys. B* **16**, 749 (1983).
 [18] S. L. Coffey, A. Deprit, B. Miller, and C. A. Williams, *Ann. N. Y. Acad. Sci.* **497**, 22 (1987).
 [19] C. Delaunay, *Theorie du Mouvement de la Lune*, Vol. 1 [*Mém. Acad. Sci. Paris XXVIII* (1860); also Vol. 2 [XXIX (1867)]].

- [20] Y. Alhassid, E. A. Hinds, and D. Meschede, *Phys. Rev. Lett.* **59**, 1545 (1987).
- [21] E. G. Kalnis, W. Miller, and P. Winternitz, *Siam J. Appl. Math.* **30**, 630 (1976).
- [22] P. Kustaanheimo and E. Stiefel, *J. Reine Angew. Math.* **218**, 204 (1965).
- [23] E. L. Stiefel and G. Scheifele, *Linear and Regular Celestial Mechanics* (Springer-Verlag, Berlin, 1971).
- [24] M. Kuwata, A. Harada, and H. Hasegawa, *J. Phys. A* **23**, 3227 (1990).
- [25] E. U. Condon and H. Odabasi, *Atomic Structure* (Cambridge University Press, New York, 1980).
- [26] M. Kibler and T. Negadi, *Lett. Nuovo Cimento* **37**, 225 (1983).
- [27] M. Boiteux, *Physica* **65**, 381 (1973).
- [28] D. Delande and J. C. Gay, in *The Hydrogen Atom*, edited by G. F. Bassani, M. Inguscio, and T. W. Hänsch (Springer-Verlag, Berlin, 1989), p. 323; *J. Phys. B* **17**, L335 (1984).
- [29] E. L. Sibert, J. T. Hynes, and W. P. Reinhardt, *J. Chem. Phys.* **77**, 3583 (1982).
- [30] U. Fano, F. Robicheaux, and A. R. P. Rau, *Phys. Rev. A* **37**, 3655 (1988).
- [31] W. G. Harter and C. W. Patterson, *J. Chem. Phys.* **80**, 4241 (1984); W. G. Harter, *J. Stat. Phys.* **36**, 749 (1984); W. G. Harter, *Comput. Phys. Commun.* **8**, 319 (1988).
- [32] R. N. Zare, *Angular Momentum: Understanding Spatial Aspects in Chemistry and Physics* (Wiley, New York, 1988).
- [33] T. Uzer, *Phys. Rev. A* **42**, 5787 (1990).
- [34] A. R. P. Rau and L. Zhang, *Phys. Rev. A* **42**, 6342 (1990).
- [35] T. P. Grozdanov and H. S. Taylor, *J. Phys. B* **19**, 4075 (1986).
- [36] M. Robnik and E. Schröder, *J. Phys. A* **18**, L853 (1985).
- [37] J. B. Delos, S. K. Knudson, and D. W. Noid, *Phys. Rev. A* **28**, 7 (1983); **35**, 5064 (1987).
- [38] W. H. Miller, *J. Chem. Phys.* **48**, 1651 (1968).
- [39] J. N. L. Connor, T. Uzer, R. A. Marcus, and A. D. Smith, *J. Chem. Phys.* **80**, 5095 (1984).

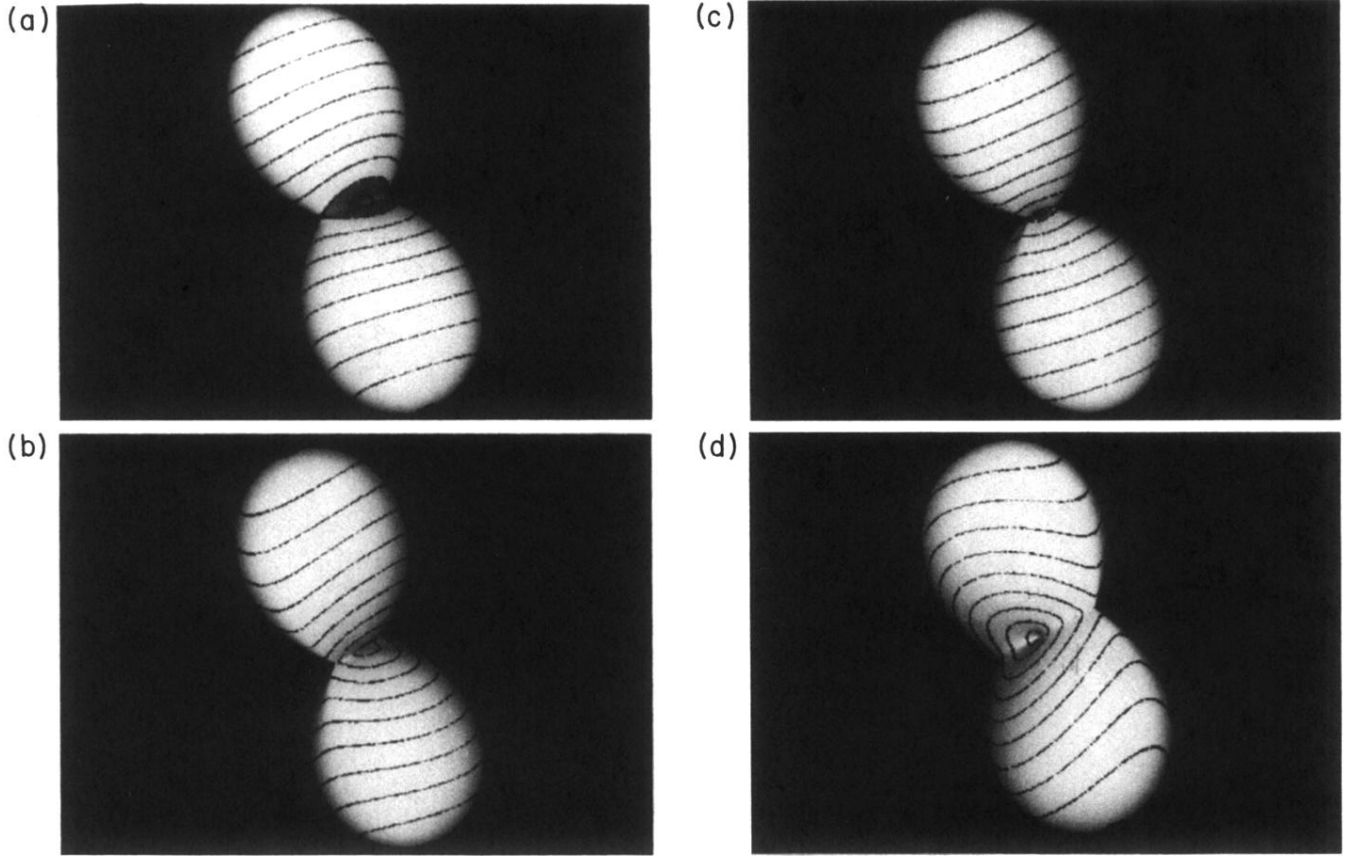


FIG. 4. Rotational energy surfaces corresponding to $n=23$ and (a) $m=0$, (b) $m=4$, (c) $m=n/\sqrt{5}$, and (d) $m=22$. The surfaces have been shaded gray to indicate where Λ is negative. The Cartesian coordinate system is defined as follows using (a). One axis runs along the long axis of the body. A second axis around which the angle θ_z varies [see Eq. (43)] emanates from the dimple (shaded gray) in (a). The third axis is orthogonal to these. The orientation is kept constant between figures. The contours are level curves corresponding to the intersection of the RES with spheres of progressively increasing radii equal to $|\Lambda|$.